Available online at www.sciencedirect.com

ScienceDirect

Energy Reports 6 (2020) 709–715

www.elsevier.com/locate/egyr

a2020 7th International Conference on Power and Energy Systems Engineering (CPESE 2020), 26–29 September 2020, Fukuoka, Japan

An improved indirect instantaneous torque control strategy of switched reluctance motor drives for light electric vehicles

Mahmoud Hamouda[a,b,*], Amir Abdel Menaem[c], Hegazy Rezk[d,e], Mohamed N. Ibrahim[f,g,h], László Számel[b]

[a] *Electrical Engineering Department, Mansoura University, 35516 Mansoura, Egypt*

[b] *Department of Electric Power Engineering, Budapest University of Technology and Economics, H-1521 Budapest, Hungary*

[c] *Department of Automated Electrical Systems, Ural Power Engineering Institute, Ural Federal University, 620002 Yekaterinburg, Russia*

[d] *College of Engineering at Wadi Addawaser, Prince Sattam Bin Abdulaziz University, 11991 Wadi Aldawaser, Saudi Arabia*

[e] *Electrical Engineering Department, Faculty of Engineering, Minia University, 61111 Minia, Egypt*

[f] *Electrical Engineering Department, Kafrelshiekh University, Kafr el-Sheikh 33511, Egypt*

[g] *Department of Electromechanical, Systems and Metal Engineering, Ghent University, Ghent 9000, Belgium*

[h] *FlandersMake@UGent – corelab EEDT-MP, 3001 Leuven, Belgium*

Received 30 October 2020; accepted 15 November 2020

Abstract

The switched reluctance motors (SRMs) are powerful alternatives for electric vehicles (EVs). However, the high torque ripple is the main obstacle for their acceptance in high-performance applications. This paper introduces an improved indirect instantaneous torque control (IITC) strategy of SRMs for EVs. It aims to achieve the vehicle requirements including maximum torque per ampere (MTPA), minimum torque ripple, high efficiency, and extended speed range. First, a simple analytical formulation that determines the most efficient turn-on angle for torque production is developed. Second, A modified torque sharing function (TSF) is introduced to compensate for torque tracking errors. To accurately represent the SRM, its magnetic characteristics are calculated using finite element method (FEM). They are employed to build machine model and implement the required transformations. Finally, the particle swarm optimization (PSO) algorithm is adopted to determine the best control parameters for the conventional IITC. This is done basically for comparison and verification purposes. The results show the feasibility and effectiveness of the proposed control over extended speed range.

Peer-review under responsibility of the scientific committee of the 7th International Conference on Power and Energy Systems Engineering, CPESE, 2020.

Keywords: Switched reluctance motor; Direct instantaneous torque control; MTPA; TSF; Optimization; Switching angles

* Corresponding author at: Electrical Engineering Department, Mansoura University, 35516 Mansoura, Egypt.
E-mail address: m_hamouda26@mans.edu.eg (M. Hamouda).

https://doi.org/10.1016/j.egyr.2020.11.142

Peer-review under responsibility of the scientific committee of the 7th International Conference on Power and Energy Systems Engineering, CPESE, 2020.

1. Introduction

Because of their numerous advantages such as simple structure, high efficiency, high reliability, fault tolerant, control flexibility, the switched reluctance motors (SRMs) are good candidates for electric vehicles (EVs) [1–3]. However, the high torque ripple is the major drawback of SRM. It causes oscillation and noise of vehicle body. Hence, it has to be treated carefully [4,5].

Several researches have been directed to reduce the torque ripple based on machine design [6], and/or control techniques [7]. The machine design is effective only over a limited speed range. Besides, it decreases the torque density as the air-gap which is not an option for EVs [8]. The current or flux profiling can reduce torque ripple over a wider speed range, but still limited [9]. Besides, it requires extensive and time time-consuming pre-calculations to determine the optimal current or flux profiles. As a result, the instantaneous torque control (ITC) techniques are gaining a huge interest for reducing torque ripples of SRMs. They vary the current at each sample time providing high control flexibility to reduce torque ripple and improve drive efficiency [10]. Among these techniques, the indirect ITC (IITC) based on torque sharing function (TSF) is an effective and promising strategy for torque ripple reduction of SRM drives. The torque is controlled indirectly by controlling phase current profile. The IITC employs TSFs to distribute the torque between motor phases aiming to have a total free-ripple torque. The main objective of TSF is maintaining torque sharing and minimum torque ripple. However, the TSF is meant only for low speed operation because of the limited dc voltage; they also provides a lower torque to current ratio [1]. Therefore, many TSFs have been proposed to achieve a secondary objective [10]. The secondary objective could be minimizing copper losses, enhancing torque–speed capability, or increasing efficiency. In [11], an offline TSF is proposed to extend the torque–speed range of SRM. It aims to minimize the copper losses and the rate-of-change-of-flux-linkage (RCFL). In [5], an online TSF is proposed to overcome the limitations of offline TSF. The total torque is determined by the phase with the lower absolute RCFL. The compensation of tracking errors for the current and torque signals have also been reported aiming to reduce torque ripple or increasing the speed ranges. In [12], a method to compensate for the current tracking errors in the demagnetizing-period is introduced. In [13], the error in phase torque signals is used to correct reference phase torque signals. In [14], an iterative learning control method is employed to compensate the reference current signals.

The maximum torque per ampere (MTPA) production is essential for EVs as it increases the mileage per charge. The MTPA is determined by the switching angles, turn-on (θ_{on}) and turn-off (θ_{off}) angles [15–17]. However, accurate, adequate, and simple methods to estimate properly the switching angles (θ_{on}, θ_{off}) in real-time processors become a demanding task due to the continuous change of operating point in traction application and the importance of switching angles (θ_{on}, θ_{off}) on motor performance. In [15], the best θ_{on} for torque production is estimated by a closed-loop control. Despite the closed-loop control provides high performance over wide speed range, it is a complicated method for real-time implementation. Therefore, analytical methods are developed to determine the best switching angles as they offer simple and fast solutions [16,17].

This paper presents an improved IITC based on TSF strategy of SRM drives for EVs. It aims to achieve the vehicle requirements of MTPA, minimum torque ripples, high efficiency, and wide speed range. First, the MTPA based IITC is introduced. A simple analytical formulation is developed to achieve the MTPA conditions. The analytical solution suits the continuous change of operating point for an EV. Besides, it simplifies the control algorithm for real-time implementation and reduces the cost. The torque data, obtained from finite element method (FEM), are used to develop the required torque to current transformations. Second, the torque error is estimated. Then, it is compensated within the TSF. The modified TSF compensates torque error with the incoming phase as it has the minimum rate of change of flux linkage. The modified TSF still has a simple structure as the conventional TSFs.

The paper organization is done as follows: the machine modeling is included in Section 2. The proposed control, the MTPA, the modified TSF are involved in Section 3. The simulation verification is given in Section 4. Finally, the conclusion is given in Section 5.

2. Machine modeling

The doubly salient structure of SRM causes not only high nonlinearities in the magnetic characteristics but also makes the flux $\lambda(i, \theta)$, torque $T(i, \theta)$, and inductance $L(i, \theta)$ functions of current (i) and position (θ). The voltage (v) and torque (T_e) equations are given by (1) [18]. To accurately model the SRM considering saturation

and nonlinearities, the FEM is used to calculate the magnetic characteristics. The calculated magnetic characteristics using FEM are given in Fig. 1. Table 1 includes the motor geometrical dimensions.

$$v = Ri + \frac{\partial \lambda(i,\theta)}{\partial t}; \quad \lambda(i,\theta) = L(i,\theta)\, i; \quad T(i,\theta) = \frac{1}{2}\frac{\partial L(i,\theta)}{\partial \theta} i^2; \quad T_e = \sum T(i,\theta) \tag{1}$$

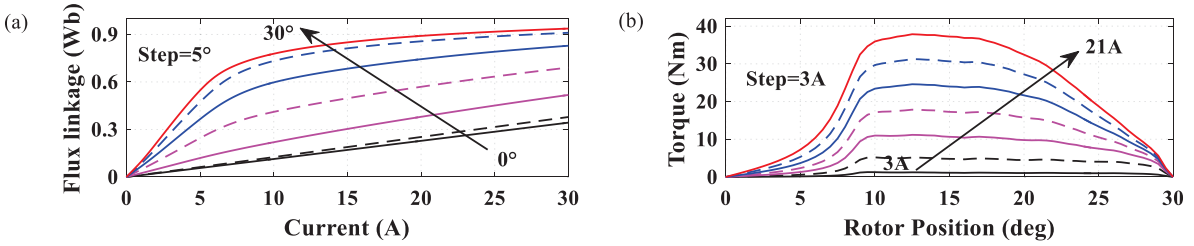

Fig. 1. The FEM-calculated magnetic characteristics: (a) the flux; (b) the torque.

Table 1. The design data of 8/6 SRM prototype in *mm*.

Geometry parameter	Value	Geometry parameter	Value
Output power (kW)	4.0	Height of rotor/stator pole	18.1/29.3
Rated voltage (v)	600	Outer stator/rotor diameters	179.5/96.7
Rated speed (r/min)	1500	Rotor/stator pole arcs	21.5°/20.45°
Air-gap length	0.4	Stack length	151

3. The proposed IITC strategy

Fig. 2(a) illustrates the block diagram of conventional IITC. As noted, it has a medium loop torque controller. The torque controller uses a TSF to distribute total reference torque (T_{ref}) among motor phases. The output of TSF is the reference torque for each phase (T_{ph-ref}). The torque inverse model *i(T, θ)* is employed to generate the reference current signals (i_{ph-ref}) from T_{ph-ref}. This is not a straightforward transformation; it is achieved based on the FEM-calculated torque characteristics in form of lookup tables. The conventional IITC is used for comparison and verification. Hence, the optimum control parameters for conventional IITC are estimated numerically using particle swarm optimization (PSO). The PSO is employed to estimate the optimum control parameters that achieves minimum torque ripples (T_r) and minimum RMS current (I_{RMS}). The minimum I_{RMS} leads to MTPA. The objective function (F_{obj}) of PSO is given by (2). The goal is to minimize F_{obj} that leads to the minimum T_r and the minimum I_{RMS}. T_{rb} and I_{RMSb} are the base values for the torque ripple and the current, respectively. w_r and w_c are the weight factors of torque ripple and current, respectively. w_r is set to 0.6 and w_c is set to 0.4.

$$F_{obj}(\theta_{on}, \theta_{ov}) = min\left(w_r \frac{T_r}{T_{rb}} + w_c \frac{I_{RMS}}{I_{RMSb}}\right); \quad w_r + w_c = 1 \tag{2}$$

The proposed IITC is given in Fig. 2(b). It involves two improvements. First, it uses an analytical formulation to determine the most efficient angles for torque production (MTPA). Second, it compensates the torque ripples aiming to extend the operating speed range. The details of control design are given below.

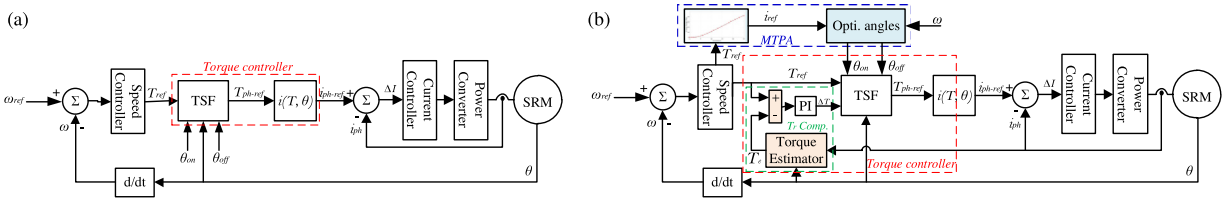

Fig. 2. (a) the conventional IITC; (b) the proposed IITC.

3.1. Maximum Torque per Ampere (MTPA)

The MTPA for SRM drives is achieved with the proper estimation of switching angles (θ_{on}, θ_{off}). For IITC strategies, the conduction angle (θ_c) is constant (for 8/6 SRM $\theta_c = 15°$). Hence, $\theta_{off} = \theta_{on} + 15°$. Therefore, θ_{on} is the dominant parameter for torque production. Now, the MTPA means the determination of optimum θ_{on} that extracts the maximum possible torque of SRM under the same current level. Because of the high nonlinearity of SRMs, the extraction of maximum possible torque is done based on the analysis and observation of static torque curves (obtained from FEM) [15–17]. As concluded, the best torque production can be obtained when the first peak of phase current reaches reference current at angle θ_m [15–17]. θ_m is the starting point of increasing inductance zone.

From (1) with $\lambda(i, \theta) = L(i, \theta)i$, the voltage equation becomes as follows:

$$v = Ri + \frac{\partial}{\partial t} L\,(i,\theta)\, i = Ri + L\,(i,\theta)\,\frac{di}{dt} + i\frac{dL\,(i,\theta)}{d\theta}\frac{d\theta}{dt} = Ri + L\,(i,\theta)\,\frac{di}{dt} + ik_b\omega \tag{3}$$

where $k_b = dL(i, \theta)/d\theta$ and $\omega = \mathrm{d}\theta/dt$.

Solving (3) for the current (i), then for the rise time (t_r) is illustrated by (4). For MTPA, the θ_{on} should be calculated backward for θ_m as illustrated by (5).

$$i\,(t) = \frac{V_{DC}}{R + k_b\omega}\left[1 - e^{-\left(\frac{R+k_b\omega}{L_u}\right)t_r}\right]; \quad t_r = \frac{-L\,(i,\theta)}{R + k_b\omega} ln\left(1 - i_{ref}\frac{R + k_b\omega}{V_{DC}}\right) \tag{4}$$

$$\theta_{on} = \theta_m - \omega t_r = \theta_m + \frac{L_u}{R + k_b\omega} ln\left(1 - i_{ref}\frac{R + k_b\omega}{V_{DC}}\right) \tag{5}$$

where R is the phase resistance, V_{DC} is the dc-link voltage.

To simplify the control algorithm as well as considering accurately the effect of back-emf voltage, L_u is calculated as the average value of phase inductance $L(i, \theta)$ over minimum inductance zone [0, θ_m]. k_b is also calculated as the average value over this zone. Therefore, the optimum θ_{on} is estimated as a function ω and i_{ref}. Since i_{ref} is not an available signal in conventional IITC of Fig. 2(a). A simple analytical torque to current transformation is introduced.

The torque (T_{ref}) to current (i_{ref}) transformation is achieved based on the torque data under MTPA conditions. Since the best torque production is achieved starting from angle θ_m, and the conduction angle is constant of 15° . The best interval for torque production is over [θ_m, θ_m+15°] as shown in Fig. 3(a). Thus, for a given current level, the average torque can be estimated directly over this interval. Then, a simple polynomial can be used to fit current against torque. The data of average torque versus current are shown in Fig. 3(b). Once, the current is available, the switching angles can be calculated as a function of motor speed and reference current using (5).

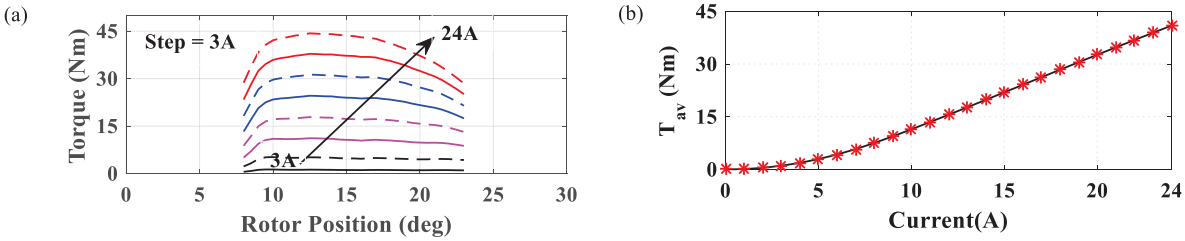

Fig. 3. Torque to current conversion. (a) torque curves over the most efficient 15°; (b) average torque vs. current.

3.2. Compensation of torque ripple

The TSF is meant only for low speed operation. After that, the torque ripple increases significantly with increases the speed due to the limited dc-link voltage [5]. The most ripple part occurs in the demagnetizing zone. In this zone, the phase current fails tracking its reference current due to the high inductance values. The fail tracking of current produces torque tracking error. In the proposed IITC of Fig. 2(b), the instantaneous motor torque (T_e) is estimated online using the torque estimator based on the fitting of FEM-calculated torque data [18]. Then, it is subtracted from T_{ref} and processed with a PI controller to generate the torque error (ΔT). After that, ΔT is compensated within the

TSF. This error (ΔT) is compensated with incoming phase using a modified TSF as given by (6). The sinusoidal TSF is adopted in this paper as it is the optimal TSF to provide minimum RMS current and rate of change of flux linkage [10].

$$TSF(\theta) = \begin{cases} 0, & if \ \ (0 \le \theta \le \theta_{on}) \\ \frac{T_e}{2} - \frac{T_e}{2} cos \frac{\pi}{\theta_{ov}} (\theta - \theta_{on}) + \Delta T, & if \ (\theta_{on} \le \theta \le \theta_{on} + \theta_{ov}) \\ T_e + \Delta T, & if \ (\theta_{on} + \theta_{ov} \le \theta \le \theta_{off}) \\ T_e - \left(\frac{T_e}{2} - \frac{T_e}{2} cos \frac{\pi}{\theta_{ov}} (\theta - \theta_{on}) \right), & if \ (\theta_{off} \le \theta \le \theta_{off} + \theta_{ov}) \\ 0, & if \ (\theta_{off} + \theta_{ov} \le \theta \le \theta_p) \end{cases} \tag{6}$$

where θ_p is the rotor period. θ_{ov} is the over-lap angle of TSF (θ_{ov} $\le$0.5θ_p - θ_{off}).

4. Results and discussion

To show the high-fidelity and effectiveness proposed control, the steady-state and the dynamic results are included compared to the conventional IITC. Noting that the control parameters for conventional IITC are optimized using PSO. Hence, they provide the best control performance for the conventional IITC strategy.

The performance indices involve the torque ripple (T_r), average torque (T_{av}), average supply current (I_{av}), root mean square of supply current (I_{RMS}), and efficiency (η). These indices are calculates as follows [1].

$$T_{av} = \frac{1}{\tau} \int_0^\tau T_e(t) dt; \quad T_r = \frac{T_{max} - T_{min}}{T_{av}}; \quad I_{av} = \frac{1}{\tau} \int_0^\tau i_s(t) dt; \quad I_{RMS} = \sqrt{\frac{1}{\tau} \int_0^\tau i^2(t) dt}; \quad \eta = \frac{\omega T_{av}}{V_{DC} I_{av}} \tag{7}$$

where τ is the time of one electric cycle. T_{max} and T_{min} are the maximum and minimum values of instantaneous torque. i_s is the instantaneous supply current. ω is the motor speed.

Fig. 4 shows the steady-state comparison between the proposed and conventional IITC strategies. The motor is tested under full load conditions. Below base speed (1500 r/min), the motor gives its rated torque (26 Nm). Above base speed, the motor torque decreases with increasing the speed as the motor outputs constant power as shown in Fig. 4(a). As noted, the proposed control provides the lowest torque ripple as seen in Fig. 4(b). Besides, it can expand the low-ripple speed-range beyond base speed up to 2250 r/min. Moreover, it succeeded to maintain the same efficiency as seen in Fig. 4(c). Furthermore, it provides a good torque to current ratio as given in Fig. 4(d).

Fig. 5 shows the dynamic performance under sudden changes in loading torque and reference speed. At 1.0 s, the reference speed is varied from 1000 r/min to 2000 r/min. Besides, at 0.7 s, the loading torque is reduced from 20 Nm to 15 Nm. As noted, a good speed tracking behavior is noted in both cases as seen in Fig. 5(a). The variation of θ_{on} is shown in Fig. 5(b). The conventional control has a smooth variation for θ_{on} that help to provide better drive-ability with noise reduction. The total generated torque is shown in Fig. 5(c). Fast dynamics and smooth torque profiles can be noticed. The proposed IITC has the minimum value of torque ripple over the whole speed-range as illustrated in Fig. 5(d). It is obvious that for the same torque ripple value, the proposed IITC has an extended-speed range. It also maintains a very good efficiency as shown in Fig. 5(c). Besides, it provides a good torque to current ratio as seen in Fig. 5(f).

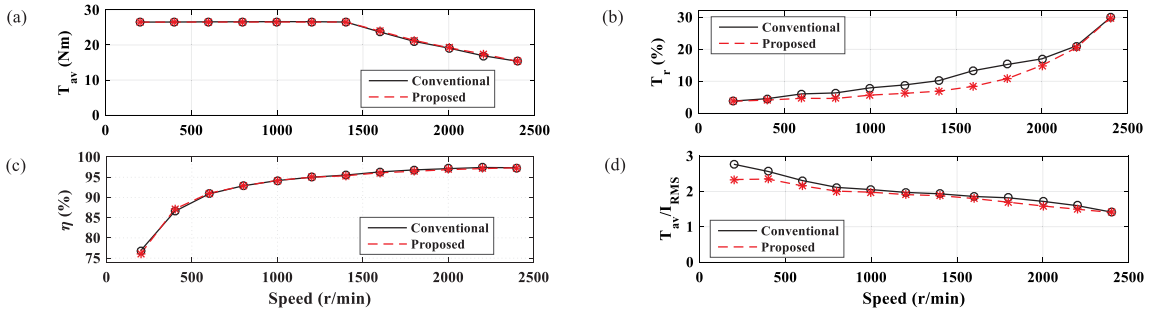

Fig. 4. The steady-state results of the proposed control compared to PSO-based control method.

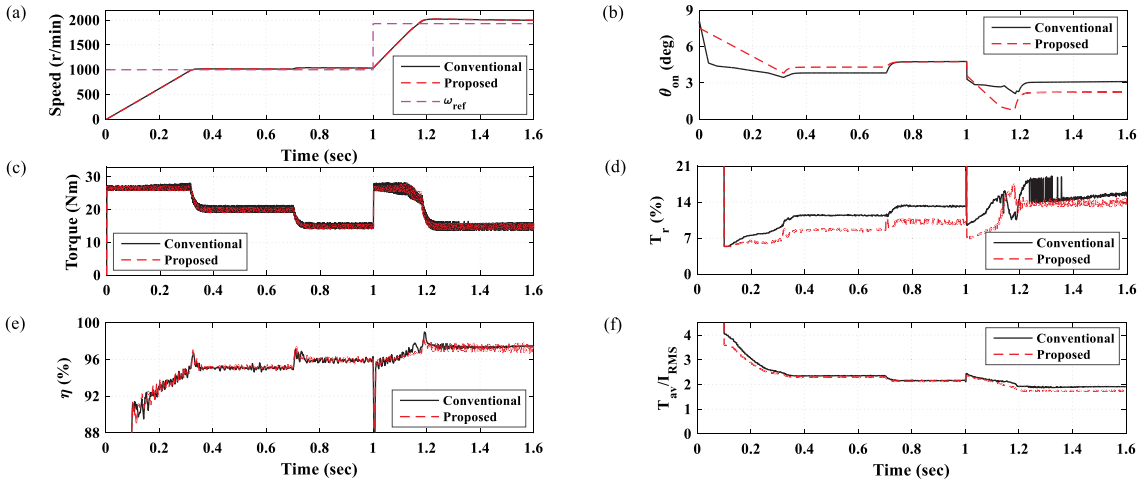

Fig. 5. The dynamic simulation results.

5. Conclusions

This paper presents an improved IITC strategy of SRM drives for light EVs. The proposed control focuses to achieve the vehicle requirements including MTPA, minimum torque ripple, high efficiency, and extended speed range. An online analytical formulation is used to determine the most efficient turn-on (θ_{on}) angle for torque production. A simple analytical method is introduced to estimate the reference current signal from torque data. Moreover, a modified TSF is introduced to compensate for torque ripple in demagnetizing period. The simulation results show that the proposed control can effectively reduce torque ripple over wider speed range. Besides, it has a simple construction and easy to implement. Moreover, it provides a very good efficiency and torque to current ratio compared to the conventional control.

Declaration of competing interest

The authors declare that they have no known competing financial interests or personal relationships that could have appeared to influence the work reported in this paper.

References

[1] Hamouda M, Abdel Menaem A, Rezk H, Ibrahim MN, Számel L. Numerical estimation of switched reluctance motor excitation parameters based on a simplified structure average torque control strategy for electric vehicles. Mathematics 2020;8(8):1213–33.
[2] Hamouda M, Számel L. Optimum control parameters of switched reluctance motor for torque production improvement over the entire speed range. Acta Polytech Hung 2019;16(3):1–20.
[3] Ibrahim MN, Sergeant P, Rashad EM. Relevance of including saturation and position dependence in the inductances for accurate dynamic modeling and control of SynRMs. IEEE Trans Ind Appl 2017;53(1):151–60.
[4] Hamouda M, Számel L. Reduced torque ripple based on a simplified structure average torque control of switched reluctance motor for electric vehicles. In: 2018 international IEEE conference and workshop in óbuda on electrical and power engineering; 2018. p. 109–14.
[5] Ye J, Bilgin B, Emadi A. An extended-speed low-ripple torque control of switched reluctance motor drives. IEEE Trans Power Electron 2015;30(3):1457–70.
[6] Chen H, Yan W, Gu JJ, Sun M. Multiobjective optimization design of a switched reluctance motor for low-speed electric vehicles with a Taguchi-CSO algorithm. IEEE/ASME Trans Mechatronics 2018;3(4):1762–74.
[7] Cheng H, Chen H, Ma L, Yu G. Research on switched reluctance machine drive topology and control strategies for electric vehicles. Turk J Electr Eng Comput Sci 2016;590–604.
[8] Moallem M, Ong CM, Unnewehr LE. Effect of rotor profiles on the torque of a switched-reluctance motor. IEEE Trans Ind Appl 1992;28(2):364–9.
[9] Mikail R, Husain I, Sozer Y, Islam MS, Sebastian T. Torque-ripple minimization of switched reluctance machines through current profiling. IEEE Trans Ind Appl 2013;49(3):1258–67.
[10] Vujičić VP. Minimization of torque ripple and copper losses in switched reluctance drive. IEEE Trans Power Electron 2012;27(1):388–99.

[11] Ye J, Bilgin B, Emadi A. An offline torque sharing function for torque ripple reduction in switched reluctance motor drives. IEEE Trans Energy Convers 2015;30(2):726–35.
[12] Chithrabhanu A, Vasudevan K. Online compensation for torque ripple reduction in SRM drives. In: 2017 IEEE transportation electrification conference, ITEC-India 2017, 2018-Janua; 2018. p. 1–6.
[13] Sun Q, Wu J, Gan C, Hu Y, Si J. OCTSF for torque ripple minimisation in SRMs. IET Power Electron 2016;9(14):2741–50.
[14] Sahoo SK, Panda SK, Xu JX. Indirect torque control of switched reluctance motors using iterative learning control. IEEE Trans Power Electron 2005;20(1):200–8.
[15] Sozer Y, Torrey DA, Mese E. Automatic control of excitation parameters for switched-reluctance motor drives. IEEE Trans Power Electron 2003;18(2):594–603.
[16] Xu YZ, Zhong R, Chen L, Lu SL. Analytical method to optimise turn-on angle and turn-off angle for switched reluctance motor drives. IET Electr Power Appl 2012;6(9):593–603.
[17] Hamouda M, Számel L. A new technique for optimum excitation of switched reluctance motor drives over a wide speed range. Turk J Electr Eng Comput Sci 2018;26(5):2753–67.
[18] Hamouda M, Számel L. Accurate magnetic characterization based model development for switched reluctance machine. Period Polytech Electr Eng Comput Sci 2019;63(3):202–12.